Figure S1

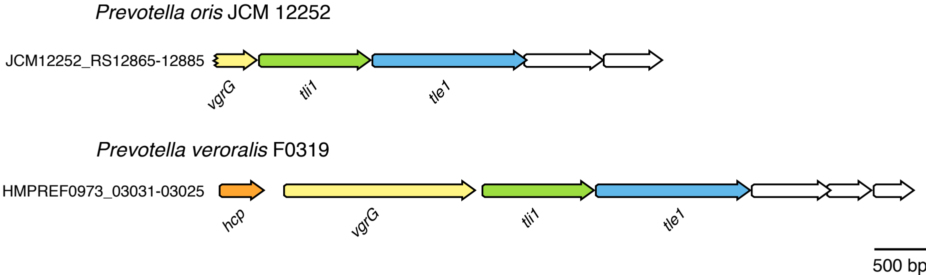

Figure S1. **Genes encoding previously identified T6SS effector proteins are found within the Bacteroidetes in similar genomic contexts as their Proteobacterial homologs. Related to Figure 1.** Genomic organization of genes encoding type VI lipase effector family 1 (Tle1) members in the Bacteroidetes *P. oris* and *P. veroralis*. ORFs encoding predicted immunity proteins (type VI lipase immunity family 1, Tli1), and elements of the T6SS (VgrG, Hcp) are noted. Analogous genes are matched in color.

Figure S2

A

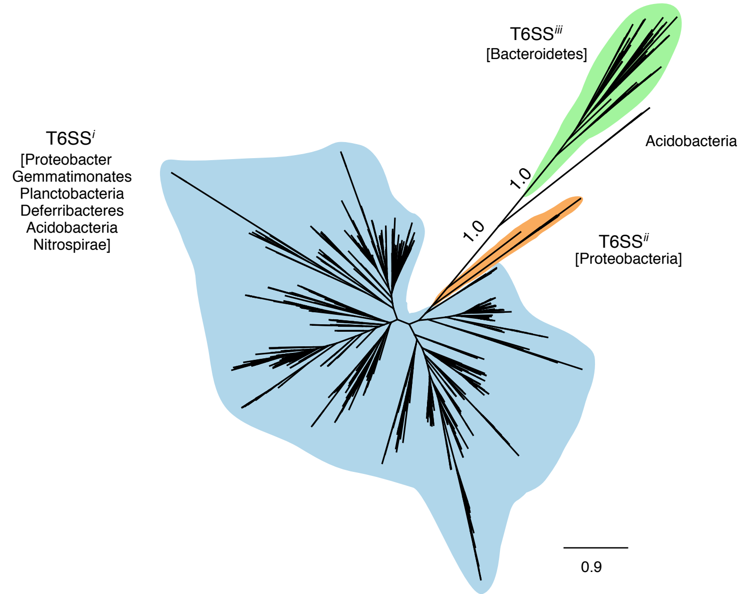

B

Granulicella mallensis MP5ACTX8

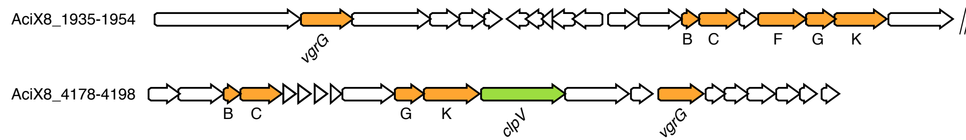

Acidobacteriaceae bacterium TAA166

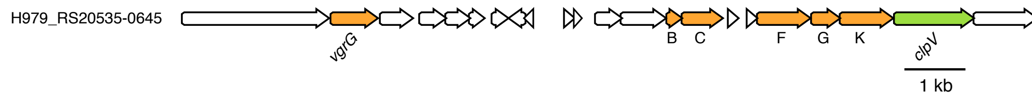

Figure S2. Phylogenetic analysis of TssF homologs and genomic context of Acidobacterial T6SS^{iii}-like proteins supports the assignment of T6SS^{iii} as phylogentically distinct from T6SS^{i-ii} and restricted to the phylum Bacteroidetes. Related to Figure 2. (A)ML phylogentic tree generated from a partial alignment of 881 representative TssF sequences spanning the diversity present in T6SS^{i-iii} gene clusters. Phyla represented by each system are indicated. Branch support values derived from aBayes analysis for the T6SS^{iii} clade are shown. Scale bar represents amino acid changes per site. (B) Genomic context of Acidobacterial proteins closely homologous to T6SS^{iii} components. Genes with commonly used *tss* nomenclature are abbreviated to a single letter, and are colored identically to Figure 1A. Genes with commonly used *tss* nomenclature are abbreviated to a single letter.

Figure S3

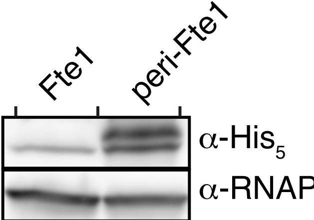

Figure S3. Both Fte1 and peri-Fte1 are expressed. Related to Figure 3. Western blot analysis performed on *E. coli* containing expression vectors for Fte1–H_6 or Fte1–H_6 directed to the periplasm (peri) under induction identical to Figure 3B. RNA polymerase (RNAP) was used as a loading control.

Figure S4

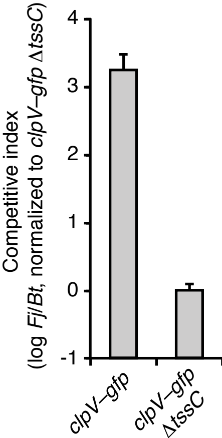

Figure S4. ***F. johnsoniae clpV–gfp* maintains T6SS^{iii} function. Related to Figure 4.** Growth competition experiments measuring fitness of the indicated *F. johnsoniae* strains in co-culture with *B. thailandensis* for 20 hours. Experiments were performed under contact-promoting conditions. Error bars represent ± SD (n = 3).

Table S1. Summary of elements conserved in T6SS^{iii} gene clusters. Related to Figure 1

Name	*F. johnsoniae* locus[a]	*B. fragilis* locus	Predicted Localization[b]	Present in T6SS^{i}	Pfam annotation[c]
VgrG	Fjoh_3260	BF9343_1930	Cytoplasmic	Yes	Phage GPD, Phage base V
ClpV	Fjoh_3281	BF9343_1940	Cytoplasmic	Yes	AAA, AAA-2, ClpB D2-small
TssB	Fjoh_3267	BF9343_1942	Cytoplasmic	Yes	None
TssC	Fjoh_3266	BF9343_1941	Cytoplasmic	Yes	DUF877
TssE	Fjoh_3263	BF9343_1932	Cytoplasmic	Yes	GWP gp25
TssF	Fjoh_3254	BF9343_1931	Cytoplasmic	Yes	None
TssG	Fjoh_3278	BF9343_1923	Cytoplasmic	Yes	DUF1305
TssK	Fjoh_3269	BF9343_1924	Cytoplasmic	Yes	None
TssN	Fjoh_3277	BF9343_1925	Inner-membrane	No	None
TssO	Fjoh_3268	BF9343_1921	Inner-membrane	No	None
TssP	Fjoh_3280	BF9343_1920	Inner-membrane	No	PKD domain
Hcp	Fjoh_3262	BF9343_1935	Cytoplasmic	Yes	None

[a]Locus tag within *F. johnsoniae* UW101 or *B. fragilis* NCTC 9343. If paralogs exist only one is indicated.
[b]Predicted localization derived from SignalP 4.1 and TMHMM 2.0 analysis of *F. johnsoniae* proteins.
[c]Analysis of *F. johnsoniae* proteins by the Pfam server (http://pfam.xfam.org/)

Table S2. Summary of proteins identified in *F. johnsoniae* secretome studies. Related to Table 1.

Movie S1. ClpV-GFP forms dynamic foci in wild-type *F. johnsoniae*. Related to Figure 4. Time-lapse fluorescence microscopy of *F. johnsoniae clpV–gfp*. The movie was collected over 6 minutes with a 5 second frame-rate.

Movie S2. Inactivation of T6SS^{iii} through a deletion of *tssC* abrogates ClpV-GFP focus formation. Related to Figure 4. Time-lapse fluorescence microscopy of *F. johnsoniae clpV–gfp* Δ*tssC*. The movie was collected over 6 minutes with a 5 second frame-rate.

File_S1 (text file; relates to Figures 1 and 2). All sequence alignments pertinent to this study.

File_S2 (Nexus file; relates to Figure 2). Full TssC tree with branch-support values.

File_S3 (Nexus file; relates to Figure 2). Full TssF tree with branch-support values.

File_S4 (Nexus file; relates to Figure 2). Tree of T6SS^{iii} TssC sequences with Acidobacterial sequences as an outgroup and all branch-support values.

Supplemental Experimental Procedures

Bacterial strains and growth conditions

F. johnsoniae, *B. thailandensis*, *P. putida*, *B. fragilis*, *B. eggerthii*, and *B. thetaiotaomicron* used in this study were derived from the sequenced strains UW101, E264, KT2440, NCTC 9343, ATCC 27754, and VPI-5482 respectively (Kim et al., 2005; McBride et al., 2009; Nelson et al., 2002; Xu et al., 2003). *E. coli* strains used in this study included DH5α for plasmid maintenance and tri-parental conjugation of plasmids into *F. johnsoniae* and *B. fragilis*, Rosetta 2(DE3) (EMD Millipore) for toxicity experiments, BL21(DE3) pLysS for the expression and purification of Fjoh_3262, and Nissle 1917 for mouse colonization experiments. *F. johnsoniae* was grown on modified tryptone yeast extract media (TYE, 10g tryptone, 5g yeast extract, and 1g $MgSO_4$ per liter supplemented with 10 mM Tris-Cl pH 7.5) (McBride and Kempf, 1996), PY2 (2g peptone, 0.5g yeast extract per liter) (Agarwal et al., 1997), synthetic CF sputum media (SCFM) (Palmer et al., 2007), or Luria-Bertani media (LB) at 23 °C. *B. thailandensis*, *E. coli*, and *P. putida* were grown on LB at 37 °C or 30 °C (*P. putida*). All *Bacteroides* strains were cultured in liquid TYG medium (Holdeman et al., 1977) at 37 °C in a flexible anaerobic chamber (Coy Laboratory Products) containing 20% CO_2, 10% H_2, and 70% N_2. *B. eggerthii* and *B. fragilis* were additionally cultured on either brain heart infusion (BHI; Becton Dickinson) agar supplemented with 10% horse blood (Colorado Serum Co. or Quad Five), or BHI supplemented with 50 µg/mL hemin (Sigma-Aldrich) and 0.5 µg/mL menadione (MP Biomedicals), respectively. Media were supplemented with antibiotics as needed for the following organisms at the indicated concentrations: *F. johnsoniae* – erythromycin (100µg ml^{-1}), streptomycin (100 µg ml^{-1}), and kanamycin (25 µg ml^{-1}), *P. putida* – gentamycin (30 µg ml^{-1}) and irgasan (25 µg ml^{-1}), *Bacteroides* – gentamycin (200 µg ml^{-1}), tetracycline (2µg ml^{-1}), and erythromycin (10 µg ml^{-1}), and *E. coli* – carbenicillin (150 µg ml^{-1}), kanamycin (50 µg ml^{-1}), streptomycin (50 µg ml^{-1}), chloramphenicol (30 µg ml^{-1}), and trimethoprim (200 µg ml^{-1}) . Isopropyl-b-D-thiogalactoside (IPTG) and rhamnose were added in stated concentrations to media to induce expression in *E. coli*. Fluorescently labeled *B. thailandensis* and *P. putida* strains possessed GFP expression cassettes integrated into the *attTn7* site as described previously (Choi et al., 2005; Schwarz et al., 2010). A marked strain of *B. thetaiotaomicron* was generated by the introduction of a tetracycline resistance gene in a pNBU2 vector as previously described (Martens et al., 2008). Allelic exchange in *F. johnsoniae* was performed utilizing the method developed by McBride and colleagues, with streptomycin counter-selection performed on PY2 media instead of CYE media and all other growth steps on TYE rather than CYE (Rhodes et al., 2011). The *B. fragilis* Δ*tssC* strain was constructed using the mobilizable *Bacteroides* suicide vector pNJR6 (Stevens et al., 1990). *B. fragilis* cointegrants were selected using erythromycin, grown under non-selective conditions to allow merodiploid resolution, and individual colonies were tested for erythromycin sensitivity and subsequently screened for the mutation by PCR. The deletion was confirmed by sequencing.

DNA manipulations

The creation, maintenance and transformation of plasmid constructs followed standard molecular cloning procedures. All primers used in this study were obtained from Integrated DNA Technologies. DNA amplification was carried out using Phusion (New England Biolabs) in HF

buffer with the addition of 1mM $MgCl_2$. DNA sequencing was performed by Genewiz Incorporated. Restriction enzymes were obtained from New England Biolabs.

Plasmid construction

Plasmids used in this study included pRR51 and PNJR6 for the introduction of non-polar mutations into *F. johnsoniae* and *B. fragilis*, respectively (Rhodes et al., 2011; Stevens et al., 1990), pCP11 for complementation (Alvarez et al., 2004; McBride and Kempf, 1996), pR600 for mobilizing plasmids into *F. johnsoniae*, R751 for plasmid mobilization into *B. fragilis*, pScrhab2 for the expression of immunity proteins (Cardona and Valvano, 2005), pET29b+ (Novagen) for the expression of proteins with a C-terminal His-tag, and pET22b+ (Novagen) for the expression of proteins directed to the periplasmic space with a C-terminal His-tag. For the generation of deletion and genomic fusion constructs for *F. johnsoniae*, 2.2 kb regions flanking the locus of interest were amplified and serially cloned into pRR51 using BamHI, XbaI, and SphI sites. Similarly, the *B. fragilis* Δ*tssC* deletion construct was created by amplifying two 1.5 kb flanks upstream and downstream of the gene, joining these regions by splicing by overlap extension PCR (Warrens et al., 1997), and ligating the resulting product into pNJR6 after a SalI/BamHI digest. For the *fte1* pET29b+ expression construct, the gene was cloned using NdeI/XhoI as fusion to the C-terminal His_6 tag, and for the pET22b+ expression construct cloning was performed using BamHI/XhoI to generate a fusion to the PelB leader peptide and C-terminal His_6 tag. For the *fti1* immunity expression construct, the gene was cloned without a stop codon into pScrhaB2 with an NdeI/XbaI digest and subsequently a linker region encoding a VSV-G epitope tag and a stop codon was introduced at the 3' end of the gene. The construct for the expression of *tsi1* was described previously (Russell et al., 2011). In order to complement Fjoh_3266 (*tssC*), the predicted promoter region of the $T6SS^{iii}$ operon containing this gene was first cloned into BamHI-digested pCP11 using a BamHI/BglII digest to generate pCP11–pT6S. Into this vector, *tssC* and a 39 base pair upstream region that includes its ribosomal-binding site was cloned using a SacI/SmaI digest.

Informatic analyses

ClpV- and VgrG-like proteins from the Bacteroidetes were identified by automated annotation from NCBI blast servers (http://blast.ncbi.nlm.nih.gov/Blast.cgi) (Altschul et al., 1990). Hcp-like proteins were initially found within *F. johnsoniae* by PHYRE 2.0 (http://www.sbg.bio.ic.ac.uk/phyre2), and were thereafter identified by homology using blastp analysis (Kelley and Sternberg, 2009). Other T6SS homologs were identified in $T6SS^{iii}$ gene clusters by the application of the iterative search algorithm jackHmmer (http://hmmer.janelia.org/search/jackhmmer) on the RefSeq protein database using seed proteins obtained from *F. johnsoniae* (Finn et al., 2011; Johnson et al., 2010). After manual removal of sequences likely to represent non-T6SS components, partial sequences, bacteriophage, or pseudogenes, sequences were aligned utilizing MAFFT within Geneious set to automated strategy choice (Katoh and Standley, 2013). These sequences were then clustered using the Geneious UPGMA algorithm and representative proteins were chosen by excluding related sequences with a calculated distance of less than 0.08 residue differences per site. This representative set was then aligned using an online MAFFT server (http://mafft.cbrc.jp/alignment/server/) using the E-INS-i strategy, a BLOSUM62 scoring matrix, and a gap open penalty of 1.53 (Katoh and Standley, 2013). For TssC and TssF trees these alignments were then trimmed using TrimAl set to the automated approach optimized for

maximum-likelihood (ML) trees, and then further manually trimmed at ends to bound the alignment with regions of relatively high conservation (Capella-Gutierrez et al., 2009). From these alignments ML trees were generated using a PHYML 3.0 server (http://www.atgc-montpellier.fr/phyml/), with the LG model of substitution (Guindon et al., 2010). For the TssC ML tree consisting of only T6SS^{iii} members, the original set of sequences obtained from jackHMMER before subsequent steps was filtered to remove all proteins not resident in T6SS^{iii} clusters except for Acidobacterial sequences in T6SS^{iii}-like clusters which were maintained for use as an outgroup. This subset was then aligned using the MAFFT G-INS-i strategy. This alignment was trimmed using TrimAl, and used to generate an ML tree using PHYML 3.0 as before. All tree branch supports were generated using the aBayes method within PHYML 3.0 (Anisimova et al., 2011).

Domain prediction for Fjoh_3281 (*clpV*), Fjoh_3257 (Fte1), and Fjoh_3274 relied on automated prediction from NCBI, structure prediction from PHYRE 2.0, and hidden-markov model prediction by HMMscan and HHpred (Finn et al., 2011; Kelley and Sternberg, 2009; Soding et al., 2005). The PAAR-like region of Fjoh_3257 was further identified through HHpred analysis performed on an alignment of proteins bearing Fjoh_3257-like sequences at their N-termini. Predicted subcellular localization was obtained through use of SignalP 4.1 and TMHMM 2.0 (Krogh et al., 2001; Petersen et al., 2011).

Preparation of samples for secretome analysis

Mid-log cultures of *F. johnsoniae* UW101 and *F. johnsoniae* UW101 Δ*tssC* grown in 2ml of SCFM were pelleted, washed, and used to inoculate 215 ml of SCFM to an OD_{600} of 0.001. Cells were then grown at 23 °C to an OD_{600} of 0.3-0.4 before being pelleted by centrifugation at 6000 g for 15 min at 4 °C. To ensure complete removal of cells, the supernatant fractions were collected and spun again at 6000 g for 15 min at 4 °C. Deoxycholic acid was then added to the sample supernatants to a final concentration of 0.2 mg/mL followed by incubation on ice for 30 min. Trichloroacetic acid (TCA) was then added to a final concentration of 8% (*v*/*v*) and the samples were incubated overnight at 4 °C. Precipitated proteins were pelleted by centrifugation at 18000 *g* for 30 min at 4 °C, dissolved in 4 mL ddH_20, and re-precipitated by the addition of 32 mL of pre-chilled 100% acetone followed by incubation at -20 °C for 2 h. The precipitate was spun at 18,000 *g* for 30 min at 4 °C, the supernatants discarded, and the pellets dried by evaporation. Samples were dissolved in 100 mM ammonium bicarbonate, 8 M urea and reduced by the addition of 1 mM Tris(2-carboxyethyl)phosphine (TCEP) followed by incubation for 1 h at 37 °C. Free cysteine residues in the protein samples were alkylated by adding iodoacetamide to a final concentration of 10 mM and incubated for 30 min at room temperature in the dark. Following quenching of iodoacetamide with 12 mM *N*-acetylcysteine, samples were diluted with 100 mM ammonium bicarbonate to lower the urea concentration to 1.5 M before treating with sequencing grade trypsin (Promega) overnight at 37 °C. Peptides were diluted with 100% acetonitrile and 10% (*w*/*v*) trifluoroacetic acid (TFA) to a final concentration of 5% (*v*/*v*) and 0.1% (*w*/*v*) and applied to C18 spin columns (Pierce) that had been charged with two washes of 100% acetonitrile followed by one wash with ddH_2O. Bound tryptic peptides were washed twice in 5% (*v*/*v*) acetonitrile, 0.1% (*w*/*v*) TFA before elution with 70% (*v*/*v*) acetonitrile, 25 mM formic acid.

MS analysis of tryptic peptides

Peptide digests were analysed by electrospray ionization in the positive ion mode on a hybrid quadrupole-orbitrap mass spectrometer (Q Exactive™, Thermo Fisher, San Jose, CA). The Q Exactive was equipped with a nanoflow HPLC system (NanoAcquity; Waters Corporation, Milford, MA) fitted with a home-built helium-degasser. Peptides were trapped on a homemade 100 µm i.d. × 20 mm long pre-column packed with 200 Å particles (5µm, C18AQ; Michrom BioResources, Auburn, CA, USA). Subsequent peptide separation was performed on an in-house constructed 75 µm i.d. × 180 mm long analytical column pulled using a Sutter Instruments P-2000 CO_2 laser puller (Sutter Instrument Company, Novato, CA) and packed with 100 Å particles (5 µm, C18AQ: Michrom). For each injection, an estimated amount of 1 µg of peptide mixture was loaded onto the pre-column at 4 µL min^{-1} in water/acetonitrile (95/5) with 0.1% (*v*/*v*) formic acid. Peptides were eluted using an acetonitrile gradient flowing at 250 nL min^{-1} using mobile phase consisting of: A, water, 0.1% formic acid; B, acetonitrile, 0.1% formic acid with a total gradient time of 95 min. Ion source conditions were optimized using the tuning and calibration solution recommended by the instrument provider. Data were acquired using MS survey scans in the Orbitrap followed by data-dependent selection of the 20 most abundant precursors for tandem mass spectrometry. Singly charged ions were excluded from analysis. Data redundancy was minimized by excluding previously selected precursor ions for 60 s following their selection for tandem mass spectrometry. Data were acquired using Xcalibur, version 2.2 (Thermo Fisher). Samples were analyzed in triplicate.

Tandem mass spectra were searched for sequence matches against the UniProt *F. johnsoniae* UW101 database using MaxQuant v1.4.1.2 (Cox and Mann, 2008). The following modifications were set as search parameters: peptide mass tolerance at 6 ppm, trypsin digestion cleavage after Lys or Arg (except when followed by Pro), allowed missed cleavage site, carbamidomethylated cysteine (static modification), oxidized methionine, and protein N-term acetylation (variable modification/differential search option). Relative abundance of proteins was assessed using spectral counting (Liu et al., 2004). Proteins were filtered such that all had at least two unique peptides detected and possessed an average of three spectral counts in wild-type replicates.

Protein expression and purification

E. coli BL21 (DE3) cells (Novagen) harboring pET29b::Fjoh_3262 were grown in LB broth supplemented with kanamycin. Cells were grown at 37 °C to an OD_{600} of 0.6 before protein expression was induced with 1 mM IPTG for 4 h. Pelleted cells were then resuspended in 50 mM Tris-HCl, pH 8.0, 300 mM NaCl, 5 mM imidazole and lysed by sonication. Following centrifugation, the cleared cell lysates were passed over a Ni^{2+}-nitrilotriacetic acid affinity column using a linear gradient of 5–400 mM imidazole. The Fjoh_3262-containing fractions were then pooled and concentrated by spin ultrafiltration (10 kDa molecular weight cutoff, Amicon) before being further purified by size exclusion chromatography in 20 mM Tris-HCl, pH 8.0, 150 mM NaCl.

Negative stain electron microscopy

Purified Fjoh_3262-His_6 was negatively stained by 0.75% uranyl formate using standard procedures (Ohi et al., 2004). Images were collected on a transmission electron microscope T12 (FEI) at room temperature operating under 120 kV and recorded at a magnification of 68,000X on a 4k X 4k Teitz CCD. The size of a pixel on the displayed image is 1.50Å.

E.coli growth curves

Overnight LB cultures of *E. coli* Rosetta cells bearing the indicated plasmids were diluted 1:40 v/v in LB low salt (LB-LS, 10 g tryptone, 5 g yeast extract) without antibiotics (Figure 3B) or LB-LS supplemented with 0.1% w/v rhamnose (Figure 3C). Cells were then grown at 37 °C with shaking and measurements were taken of the optical density at 600 nm (OD_{600}) every 30 minutes. At 120 minutes cells were induced to express putative antibacterial proteins with the addition of 1 mM (Figure 3B) or 50 µM (Figure 3C) IPTG. Growth continued to be monitored every 30 minutes until the end of the experiment. Whole cell fractions for the measurement of Fte1-His_6 and peri-Fte1-His_6 expression were prepared 120 minutes after induction as described previously (Hsu et al., 2009). Western blot analysis of these fractions using anti-RNA polymerase and anti-His_6 was performed using previously defined methods (Russell et al., 2011).

Fte1 self-intoxication experiments

F. johnsoniae strains bearing the indicated mutations were streaked onto 1.5% w/v agar TYE plates 24 hours prior to the experiment. Concomitantly, 2% w/v PY2 plates were produced. On the day of the experiment PY2 plates were dried for 30 minutes open to the air and a nitrocellulose membrane was placed on the surface. *F. johnsoniae* strains were then resuspended in ddH2O to a final OD_{600} of 0.3 and 5 µl of this mixture was placed on the nitrocellulose surface. After 20 h of incubation at 23 °C cells were resuspended in ddH2O and stained with propidium iodide at final concentration of 5 µg ml^{-1} for 10 minutes. Cells were then pelleted and washed with ddH2O and readings were taken of turbidity (OD_{600}) and propidium iodide fluorescence (excitation/emission at 535/617 nm). Experiments in liquid culture were performed identically with the modification that 1 µl of cell suspension was used to inoculate 1 ml of PY2 liquid media, and after 20 h of growth 500 µl of culture was pelleted and washed in ddH2O prior to staining.

Bacterial competition experiments

For *F. johnsoniae* competition experiments, *F. johnsoniae* strains were streaked onto 1.5% w/v agar TYE plates 48 hours prior to the experiment. Cells grown from these plates were then resuspended to an OD_{600} of 0.06 in LB and 80 µl of this suspension was plated on a 1.5% w/v agar TYE plate 24 hours prior to the experiment. Concurrently, competitor cells bearing constitutive GFP reporters were streaked on LB 1.5% w/v agar plates and grown at 37 °C (*B. thailandensis*) or 30 °C (*P. putida*), and 2% agar w/v PY2 plates were generated. On the day of the experiment, the 2% agar w/v PY2 plates were dried for 30 minutes open to the air and nitrocellulose was placed on the agar surface. *F. johnsoniae* strains were respuspended from the TYE plates in ddH_2O to an OD_{600} of 3.0, and *B. thailandensis* and *P. putida* were similarly resuspended to an OD_{600} of 0.3. Suspensions were mixed at a 4:1 v/v ratio of *F. johnsoniae*:competitor and 5 µl of this solution was spotted on the nitrocellulose surface. After 20 h of growth at 23 °C competitions were harvested in 200 µl of LB and serial dilutions were generated. To obtain both initial and final counts of *F. johnsoniae* strains, dilutions were plated on TYE plates and grown at 23 °C and colonies displaying clear *F. johnsoniae* morphology were enumerated. To obtain counts of *B. thailandensis* and *P. putida*, dilutions were plated on either LB or LB supplemented with irgasan and gentamycin, and grown at 37 °C or 30 °C, respectively, selecting against *F. johnsoniae* growth. For liquid competitions, steps were performed identically except that the competition was performed in 2 ml of PY2 liquid media inoculated with either 5

µl (*B. thailandensis*) or 2.5 µl (*P. putida*) of cell suspension, and *F. johnsoniae* counts were obtained from *P. putida* co-cultures by plating on TYE supplemented with kanamycin. Visualization of competitions by photography and GFP fluorescence was performed 48 hours after the start of the experiment to allow for robust growth of GFP-labeled strains.

For *Bacteroides* growth competition experiments, all strains were grown to stationary phase in TYG medium at 37˚C anaerobically. Optical densities were adjusted to 6.0 for *B. fragilis* strains and 0.6 for the *B. thetaiotaomicron* strain bearing a tetracycline resistance gene. Cells were mixed at a 1:1 v/v ratio, pelleted, resuspended in ddH$_2$O, and 5 µl of each mixture was spotted onto nitrocellulose squares placed on BHI agar supplemented with 50 µg/mL hemin and 0.5 µg/mL menadione. After incubation at 37˚C anaerobically for 24 h, competition mixtures were resuspended in TYG medium and serial dilutions were plated on BHI agar supplemented with 10% horse blood, 200 µg/mL gentamicin, and 2 µg/mL tetracycline to select for *B. thetaiotaomicron*.

Microscopic analyses of dynamic ClpV foci

Time-lapse fluorescence microscopy sequences were acquired with a Nikon Ti-E inverted microscope fitted with a X60 oil objective, automated focusing (Perfect Focus System, Nikon), a Xenon light source (Sutter Instruments), a CCD camera (Clara series, Andor), and a custom environmental chamber as described previously (Leroux et al., 2012). NIS Elements (Nikon) was used for automated image acquisition. *F. johnsoniae* cells were prepared similarly to bacterial competition experiments with the modifications that the initial OD_{600} used was 0.75 and cells were harvested after 18h of growth as monocultures. After harvesting, cells were placed on 1.5 % w/v agarose phosphate-buffered saline pads and visualized. Automated image acquisition was performed at 5s intervals for 6 minutes.

Genomic DNA extraction

B. eggerthii and *B. fragilis* were each grown to stationary phase in 5 mL liquid TYG medium. Genomic DNA was extracted by phenol-chloroform extraction and bead-beating as described (Degnan et al., 2014).

Gnotobiotic animal studies

All animal experiments were performed using protocols approved by the Yale University Institutional Animal Care and Use Committee. Germ-free Swiss Webster mice were maintained in flexible plastic gnotobiotic isolators with a 12-hour light/dark cycle. Mice were individually caged (n = 5/group) and were provided with standard autoclaved mouse chow (5K67 LabDiet, Purina) ad libitum. On day 0, mice were gavaged orally with $2x10^8$ CFU of each strain (*B. fragilis*, *B. eggerthii*, and *E. coli*). Animals were sacrificed on day 7 and samples were collected along the length of the gut. All samples were snap-frozen in liquid nitrogen and stored at -80˚C. To obtain RNA, mouse cecum samples were resuspended in RNAprotect Bacteria Reagent (Qiagen), and subjected to bead beating for two one-minute cycles. RNA was then extracted and purified using the Trizol reagent (Invitrogen) according to the manufacturer's instructions. Contaminating genomic DNA was removed by treating RNA preparations with Turbo DNase (Invitrogen) for one hour, followed by a second Trizol purification. Prior to cDNA synthesis, RNA samples were checked for DNA contamination with PCR. From RNA samples in which no PCR product was detected after 35 cycles using primers targeting *rpoD* of *B. fragilis,* cDNA was synthesized using the iScript cDNA synthesis kit (Biorad). Quantitative PCR to measure gene

expression was performed on cDNA samples using the SsoAdvanced™ Universal SYBR® Green Supermix (Biorad), and expression for each T6SS gene was normalized to *rpoD* expression levels in the same organisms.

Supplemental References

Agarwal, S., Hunnicutt, D.W., and McBride, M.J. (1997). Cloning and characterization of the Flavobacterium johnsoniae (Cytophaga johnsonae) gliding motility gene, gldA. Proceedings of the National Academy of Sciences of the United States of America *94*, 12139-12144.

Altschul, S.F., Gish, W., Miller, W., Myers, E.W., and Lipman, D.J. (1990). Basic local alignment search tool. Journal of molecular biology *215*, 403-410.

Alvarez, B., Secades, P., McBride, M.J., and Guijarro, J.A. (2004). Development of genetic techniques for the psychrotrophic fish pathogen Flavobacterium psychrophilum. Applied and environmental microbiology *70*, 581-587.

Anisimova, M., Gil, M., Dufayard, J.F., Dessimoz, C., and Gascuel, O. (2011). Survey of branch support methods demonstrates accuracy, power, and robustness of fast likelihood-based approximation schemes. Systematic biology *60*, 685-699.

Capella-Gutierrez, S., Silla-Martinez, J.M., and Gabaldon, T. (2009). trimAl: a tool for automated alignment trimming in large-scale phylogenetic analyses. Bioinformatics (Oxford, England) *25*, 1972-1973.

Cardona, S.T., and Valvano, M.A. (2005). An expression vector containing a rhamnose-inducible promoter provides tightly regulated gene expression in Burkholderia cenocepacia. Plasmid *54*, 219-228.

Choi, K.H., Gaynor, J.B., White, K.G., Lopez, C., Bosio, C.M., Karkhoff-Schweizer, R.R., and Schweizer, H.P. (2005). A Tn7-based broad-range bacterial cloning and expression system. Nature methods *2*, 443-448.

Cox, J., and Mann, M. (2008). MaxQuant enables high peptide identification rates, individualized p.p.b.-range mass accuracies and proteome-wide protein quantification. Nature biotechnology *26*, 1367-1372.

Degnan, P.H., Barry, N.A., Mok, K.C., Taga, M.E., and Goodman, A.L. (2014). Human gut microbes use multiple transporters to distinguish vitamin B(1)(2) analogs and compete in the gut. Cell host & microbe *15*, 47-57.

Finn, R.D., Clements, J., and Eddy, S.R. (2011). HMMER web server: interactive sequence similarity searching. Nucleic acids research *39*, W29-37.

Guindon, S., Dufayard, J.F., Lefort, V., Anisimova, M., Hordijk, W., and Gascuel, O. (2010). New algorithms and methods to estimate maximum-likelihood phylogenies: assessing the performance of PhyML 3.0. Systematic biology *59*, 307-321.

Holdeman, L.V., Cato, E.D., and Moore, W.E.C. (1977). Anaerobe Laboratory Manual (Blacksburg, VA, Virginia Polytechnic Institute and State University Anaerobe Laboratory).

Hsu, F., Schwarz, S., and Mougous, J.D. (2009). TagR promotes PpkA-catalysed type VI secretion activation in Pseudomonas aeruginosa. Mol Microbiol *72*, 1111-1125.

Johnson, L.S., Eddy, S.R., and Portugaly, E. (2010). Hidden Markov model speed heuristic and iterative HMM search procedure. BMC Bioinformatics *11*, 431.

Katoh, K., and Standley, D.M. (2013). MAFFT multiple sequence alignment software version 7: improvements in performance and usability. Molecular biology and evolution *30*, 772-780.

Kelley, L.A., and Sternberg, M.J. (2009). Protein structure prediction on the Web: a case study using the Phyre server. Nature protocols *4*, 363-371.

Kim, H.S., Schell, M.A., Yu, Y., Ulrich, R.L., Sarria, S.H., Nierman, W.C., and DeShazer, D. (2005). Bacterial genome adaptation to niches: divergence of the potential virulence genes in three Burkholderia species of different survival strategies. BMC genomics *6*, 174.

Krogh, A., Larsson, B., von Heijne, G., and Sonnhammer, E.L. (2001). Predicting transmembrane protein topology with a hidden Markov model: application to complete genomes. Journal of molecular biology *305*, 567-580.

Leroux, M., De Leon, J.A., Kuwada, N.J., Russell, A.B., Pinto-Santini, D., Hood, R.D., Agnello, D.M., Robertson, S.M., Wiggins, P.A., and Mougous, J.D. (2012). Quantitative single-cell characterization of bacterial interactions reveals type VI secretion is a double-edged sword. Proceedings of the National Academy of Sciences of the United States of America *109*, 19804-19809.

Liu, H., Sadygov, R.G., and Yates, J.R., 3rd (2004). A model for random sampling and estimation of relative protein abundance in shotgun proteomics. Analytical chemistry *76*, 4193-4201.

Martens, E.C., Chiang, H.C., and Gordon, J.I. (2008). Mucosal glycan foraging enhances fitness and transmission of a saccharolytic human gut bacterial symbiont. Cell host & microbe *4*, 447-457.

McBride, M.J., and Kempf, M.J. (1996). Development of techniques for the genetic manipulation of the gliding bacterium Cytophaga johnsonae. Journal of bacteriology *178*, 583-590.

McBride, M.J., Xie, G., Martens, E.C., Lapidus, A., Henrissat, B., Rhodes, R.G., Goltsman, E., Wang, W., Xu, J., Hunnicutt, D.W., *et al.* (2009). Novel features of the polysaccharide-digesting gliding bacterium Flavobacterium johnsoniae as revealed by genome sequence analysis. Applied and environmental microbiology *75*, 6864-6875.

Nelson, K.E., Weinel, C., Paulsen, I.T., Dodson, R.J., Hilbert, H., Martins dos Santos, V.A., Fouts, D.E., Gill, S.R., Pop, M., Holmes, M., *et al.* (2002). Complete genome sequence and comparative analysis of the metabolically versatile Pseudomonas putida KT2440. Environmental microbiology *4*, 799-808.

Ohi, M., Li, Y., Cheng, Y., and Walz, T. (2004). Negative Staining and Image Classification - Powerful Tools in Modern Electron Microscopy. Biol Proced Online *6*, 23-34.

Palmer, K.L., Aye, L.M., and Whiteley, M. (2007). Nutritional cues control Pseudomonas aeruginosa multicellular behavior in cystic fibrosis sputum. J Bacteriol *189*, 8079-8087.

Petersen, T.N., Brunak, S., von Heijne, G., and Nielsen, H. (2011). SignalP 4.0: discriminating signal peptides from transmembrane regions. Nature methods *8*, 785-786.

Rhodes, R.G., Pucker, H.G., and McBride, M.J. (2011). Development and use of a gene deletion strategy for Flavobacterium johnsoniae to identify the redundant gliding motility genes remF, remG, remH, and remI. Journal of bacteriology *193*, 2418-2428.

Russell, A.B., Hood, R.D., Bui, N.K., LeRoux, M., Vollmer, W., and Mougous, J.D. (2011). Type VI secretion delivers bacteriolytic effectors to target cells. Nature *475*, 343-347.

Schwarz, S., West, T.E., Boyer, F., Chiang, W.C., Carl, M.A., Hood, R.D., Rohmer, L., Tolker-Nielsen, T., Skerrett, S.J., and Mougous, J.D. (2010). Burkholderia type VI secretion systems have distinct roles in eukaryotic and bacterial cell interactions. PLoS Pathog *6*.

Soding, J., Biegert, A., and Lupas, A.N. (2005). The HHpred interactive server for protein homology detection and structure prediction. Nucleic acids research *33*, W244-248.

Stevens, A.M., Shoemaker, N.B., and Salyers, A.A. (1990). The region of a Bacteroides conjugal chromosomal tetracycline resistance element which is responsible for production of plasmidlike forms from unlinked chromosomal DNA might also be involved in transfer of the element. Journal of bacteriology *172*, 4271-4279.

Warrens, A.N., Jones, M.D., and Lechler, R.I. (1997). Splicing by overlap extension by PCR using asymmetric amplification: an improved technique for the generation of hybrid proteins of immunological interest. Gene *186*, 29-35.

Xu, J., Bjursell, M.K., Himrod, J., Deng, S., Carmichael, L.K., Chiang, H.C., Hooper, L.V., and Gordon, J.I. (2003). A genomic view of the human-Bacteroides thetaiotaomicron symbiosis. Science *299*, 2074-2076.